Turkish Journal of Electrical Engineering & Computer Sciences

http://journals.tubitak.gov.tr/elektrik/

Research Article

Turk J Elec Eng & Comp Sci
() : –

doi:10.3906/elk-2106-80

Smart charging of electric vehicles to minimize the cost of charging and the rate of transformer aging in a residential distribution network

Arjun VISAKH*, **Manickavasagam Parvathy SELVAN**

Department of Electrical & Electronics Engineering, National Institute of Technology, Tiruchirappalli, India

Received: 15.06.2021 • **Accepted/Published Online:** 02.11.2021 • **Final Version:** ..2021

Abstract: Electric vehicles (EVs) exhibit several benefits over combustion engine vehicles, making them an attractive mode of mobility for the future. However, supplying the electrical energy required to recharge their batteries could adversely affect the power system infrastructure. The most severe impact of EV integration is expected to be on the distribution transformers, which are among the costliest equipment in the distribution network. Sustained overloads on the transformer could lead to accelerated aging and early retirement. As the rate of EV deployment rises, so does the probability of transformer overloads and the subsequent loss of life. There is a need for smart charging schemes in which the distribution system operator can schedule the charging of EVs in an optimal manner that prevents overloads and extends the transformer's life. However, EV owners might hesitate to surrender the charging control of their vehicles for the utility's benefit alone. Charging-cost minimization has been identified as an effective motivation for EV users to participate in charge management schemes. This paper presents a smart charging scheme, which minimizes the cost of charging EVs by optimizing their charging powers with respect to a real-time pricing tariff. As the electricity price changes dynamically with the system demand, cost minimization is equivalent to network decongestion. A decongested network is less susceptible to overloads and equipment damage. Simulation results show that with smart charging, the charging cost incurred by EV owners as well as the rate of aging undergone by the transformer can be significantly reduced.

Key words: Electric vehicles, smart charging, charging-cost minimization, transformer aging, hot-spot temperature

1. Introduction

Electric vehicles (EVs) have emerged as a practical solution to reduce the transportation sector's petroleum consumption and greenhouse gas emissions. EVs, if widely adopted, could play a significant role in the global efforts to curb air pollution amidst climate-change concerns. In addition to nullifying fossil-fuel requirements and tailpipe emissions, EVs can also bring down the per-kilometer cost of mobility [1]. Thus, EVs represent a mode of transportation that is both economically and environmentally beneficial while being technologically realizable. The smart grid environment with distributed energy resources and advanced metering infrastructure promises to be conducive for the effective integration of EVs.

Like any other energy storage device, the EV batteries need to be recharged periodically. Due to the limited number of public charging options, most EV users are expected to charge their vehicles at home. The addition of EV charging load can double the energy consumption of a typical household [2]. Based on the daily travel behavior exhibited by light-vehicle owners, it is anticipated that the majority of EVs will be

*Correspondence: arjunvisakh301@gmail.com

plugged into the distribution system within a narrow time frame, thereby overloading the network equipment [3]. Uncontrolled EV charging could also worsen the distribution system's power quality and energy efficiency [4]. The overloads caused by EV loads will accelerate the aging of network assets, especially the distribution transformers (DTs). Sustained overloads on the DT could raise its internal temperature significantly, causing insulation degradation and loss of life. The loss of life is exacerbated in cities with warmer climates, leading to accelerated aging, service disruption, and early retirement of DTs [5].

The flexibility of EV energy demand presents the distribution system operator (DSO) with an opportunity to centrally manage the charging of vehicles connected to an overloaded DT. Thus, the EV charging loads can be optimally scheduled with smart charging (SC) technology instead of replacing the DT with a larger unit. SC schemes for EVs could be motivated by a wide range of techno-economic objectives. EV charging may be coordinated with the objective of peak shaving [6, 7] and flattening the load profile [8, 9]. The variance of system demand from the optimal loading can be minimized with controlled charging of EVs [10, 11]. The energy losses in the system can be minimized by optimally scheduling the EV charging loads [12, 13]. SC schemes that minimize voltage deviations in the network have also been developed [14, 15]. In addition to these technical objectives, SC may also seek to minimize the utility's generation costs [16, 17] or the EV owners' charging cost [18, 19]. The bidirectional communication and smart metering that are indispensable for the above SC strategies require significant capital outlay. The loss of life of DTs, which are among the most expensive components in the grid infrastructure, is a critical factor in deciding whether to invest in SC solutions or not [20]. DT aging depends upon the thermal effects from loading. All of the SC approaches cited above have ignored the DT's thermal modeling aspects and hence fail to account for its loss of life. A brief review of the SC schemes that have taken transformer aging into consideration is given below.

A peak-shaving strategy that improves DT insulation life was presented in [21], but it ignores the randomness of EV mobility as all the vehicles are assumed to plug in and plug out simultaneously. Although the temperature-based SC scheme in [20] prevents EVs from reducing DT life, it fails to guarantee charge completion by the time of departure. The same deficiency is found in the rule-based algorithm in [22] that lowers the aging rate of DTs. The authors in [23] concluded that delaying EV charging to off-peak hours could prolong DT life. However, off-peak charging might create a new peak load in the early off-peak hours [24]. A domestic SC scheme that prevents DT overloads and accelerated aging was presented in [25]. However, it only accounts for EV penetration up to 50% and not the worst-case scenario of 100%. A centralized strategy that cooptimizes the DT's loss of life was developed in [26], but without the provision for EV users to demand the energy desired. An optimal charging scheme that minimizes the impact of EVs on the aging of a DT was introduced in [27]. However, it does not apply to domestic charging as it was designed for a commercial charging station with solar generation and battery backup. Similarly, the SC scheduler proposed in [28] focuses on an insular grid feeding industrial loads.

Thus, there is a need to minimize the DT's loss of life caused by domestic charging of EVs without compromising on the vehicles' charge fulfillment. As transformer aging is a function of its loading, setting maximum limits on the DT to prevent overloads might seem like an obvious solution to the accelerated-aging problem. However, such a tactic might lead to missing the charging deadlines of some EVs, as observed in [20, 22]. Incomplete charging is unwelcome as it could aggravate the range anxiety among EV users and deter their participation in centralized SC programs. A successful SC method should satisfy the energy requirements of all EV owners to reduce their inconvenience [20]. Thus, placing upper bounds on DT loading is not the preferred

solution. Moreover, the authors in [20] have highlighted the need for financially motivating EV owners to give up the charging control of their vehicles for the utility's sake. Charging cost minimization has been identified as a powerful incentive to elicit the participation of EV owners in charge management schemes [29, 30].

The SC scheme employed in this paper seeks to minimize the charging cost incurred by EV owners as a reward for permitting the charging of their vehicles to be controlled by the DSO. Successful completion of charging requests is ensured by placing constraints on the final battery energy while formulating the optimization problem. Cost-minimization cannot be realized under fixed tariffs, in which the electricity price remains constant throughout the day leaving no room for optimal scheduling. The scope for cost-saving exists only under dynamic tariffs, such as time-of-use and real-time pricing. Out of these, the time-of-use tariff could shorten transformer life owing to the accelerated aging during load spikes when the lower-priced electricity becomes available [20]. Hence, in this study it is assumed that the DSO employs real-time pricing tariff in the network. The electricity price is modeled as a linear function of the system demand. This proportionality ensures that by shifting EV charging from the expensive peak-load hours to the cheaper off-peak hours, the SC algorithm can regulate transformer loading and slow down the subsequent aging. The optimized loading profile ensures minimum charging cost for EV users and maximum life for the DT simultaneously. Thus, the SC scheme represents a win-win scenario for both the DSO and the EV owners. The rest of this paper is organized as follows: Section 2 presents the modeling aspects of the simulation study. The need for SC and its mathematical formulation is covered in Section 3. A method for estimating the aging of a transformer using its thermal model is explained in Section 4. The simulation results are discussed in Section 5 and the paper is concluded in Section 6.

2. Distribution system modeling

In order to account for the variations in the DT's loading and operating temperature, it is necessary to discretize the day into smaller time intervals. In this study, each day is assumed to be divided into 96 time slots, each of length $\Delta t = 0.25$ h [26]. Let $\mathbf{I}$ represent the set of intervals in a day that begins at 12 noon and ends 24 h later at 12 pm on the next day, such that, $\mathbf{I} = \{12:00\,\text{pm} - 12:15\,\text{pm}, \ldots, 11:45\,\text{pm} - 12:00\,\text{am}, 12:00\,\text{am} - 12:15\,\text{am}, \ldots, 11:45\,\text{am} - 12:00\,\text{pm}\}$. System variables, such as power flows and temperatures are assumed to remain unchanged during each time interval.

2.1. Network topology

The IEEE European low voltage test feeder[1] is used as the test system in this study. It is a radial distribution feeder operating at 416 V (phase-to-phase), which is typical in European low voltage distribution systems. This distribution network supplies single-phase electricity at 240 V to 55 residential consumers with connected load of 3 kW each. Each household's load variation over 24 h is provided with a one-minute resolution for time-series simulation. The household loads in the network correspond to lighting, cooling, heating, cooking or other domestic applications that cannot be rescheduled by the DSO. The aggregate demand of such nonschedulable loads represents the base load on the system, which is beyond the DSO's control and cannot be modified. The overall power factor of the base load is 0.9 lagging. The low-voltage feeder is connected to the medium-voltage system by a 11 kV/ 416 V, 160 kVA three-phase DT. The transformer loading during the i-th interval, L^i_{DT} consists of two parts, such that:

$$L^i_{DT} = L^i_B + L^i_{EV}. \tag{1}$$

[1]IEEE PES Distribution Systems Analysis Subcommittee. Radial Test Feeders. European Low Voltage Test Feeder [online]. Website https://site.ieee.org/pes-testfeeders/resources [accessed 18 July 2021].

The term L_B^i in (1) refers to the base load, that can be predicted by load forecasting. Thus, the value of L_B^i is assumed to be known in advance for the whole day. The term L_{EV}^i denotes the controllable EV charging load that can be rescheduled optimally by the DSO. Due to the randomness of vehicle mobility, L_{EV}^i is unpredictable and its modeling is explained in the following section.

2.2. Electric vehicle modeling

EVs utilize the energy stored in their batteries to power the electric drive. Based on the presence of auxiliary combustion engine, EVs can be categorized into hybrid electric vehicles or battery electric vehicles (BEVs). The EVs considered in this study are plug-in BEVs that can be connected to the power distribution network via standard power outlets for recharging their batteries. Four different EV models were considered in this study, with specifications[2] as indicated in Table 1. It can be seen that each vehicle model has a different battery capacity and charging efficiency. The penetration level of EVs is assumed to be 100%, i.e. all the fifty-five consumers own EVs. This situation represents the worst-case scenario in terms of DT loading and aging [26]. Let $\mathbf{N} = \{EV_1, EV_2, EV_3, \ldots, EV_{55}\}$ represent the set of all EVs, with the make of each vehicle randomly picked from Table 1. The power demand of an EV under charging depends on the maximum rating of its on-board charger, P^{max}. It is assumed to be 3 kW, which corresponds to the charging rate for plug outlets with 16 A capacity that are common in European networks [31]. The provision for transferring power from vehicle-to-grid (V2G) is not considered in this study.

Table 1. EV specifications.

EV Make/Model	Year of launch	Battery capacity (kWh)	Charger efficiency (%)
Chevrolet Volt	2012	16	88.5
BMW i3	2014	18.8	93
Nissan Leaf	2015	24	88
Mercedes B-Class	2015	36	87

The energy requirement of the n-th EV ($\forall n \in \mathbf{N}$) depends on its battery's initial energy at the time of plug-in, $E_n^{initial}$, and the desired energy at plug-out time, $E_n^{desired}$. The residual energy available in the EV battery at the start of charging is a function of the total distance travelled by the vehicle since it was last charged. The uncertainty in $E_n^{initial}$ is simulated using a normal probability distribution model with mean of 50% and standard deviation of 30% of the vehicle's battery capacity [32]. Thus, $E_n^{initial}$ is a random variable that depends on battery capacity, which in turn varies from vehicle to vehicle as evident from Table 1. It is further assumed that all the EVs are required to be fully charged by the hour of departure such that $E_n^{desired} = E_n^{capacity}$. The next parameter to be modeled is the EV's plug-in duration, which depends on the time of arrival and departure from home. Previous studies based on traffic-survey data have identified the Gaussian distribution as an effective tool to model the travel pattern of EVs [32, 33]. In this study, the arrival time is assigned a Gaussian distribution with a mean of 6 p.m. and a standard deviation of 2 hours, whereas the departure time's distribution has a mean of 7 a.m. with 2 h as standard deviation [33]. Let t_n^{arr} denote the arrival (and plug-in) time of the n-th EV and let t_n^{dep} denote its departure time. Then, the charging task of

[2]Idaho National Laboratory. Vehicle Charging System Testing [online]. Website https://avt.inl.gov/content/charging-system-testing/vehicle-charging-system-testing [accessed 21 October 2021].

the n-th EV can be characterized by the set of variables - $[t_n^{arr}, t_n^{dep}, E_n^{initial}, E_n^{desired}]$.

If t^i represents the starting time of the i-th time slot, then the connection status of the n-th EV during the i-th interval can be determined as:

$$s_n^i = \begin{cases} 0, & t^i < t_n^{arr} \\ 1, & t_n^{arr} \leq t^i < t_n^{dep} \\ 0, & t^i \geq t_n^{dep} \end{cases} \tag{2}$$

Furthermore, the energy-requirement status of the n-th vehicle during interval i can be defined as a function of its battery energy E_n^i at time t^i, as shown below:

$$e_n^i = \begin{cases} 1, & E_n^{initial} \leq E_n^i < E_n^{desired} \\ 0, & E_n^i \geq E_n^{desired} \end{cases} \tag{3}$$

The total EV charging load applied on the system can be expressed as:

$$L_{EV}^i = \sum_{n \in \mathbf{N}} s_n^i \cdot e_n^i \cdot p_n^i \quad , \quad \forall i \in \mathbf{I} \tag{4}$$

where p_n^i denotes the charging power of the n-th EV during the i-th interval. The value of p_n^i depends on the charging scheme employed, as explained in section 3.

2.3. Energy costs

In this study, the consumers are billed according to a real-time pricing tariff, in which the electricity price varies from time-slot to time-slot, reflecting the variations in system demand (and DT loading). Here the complex relationship between electricity price and power demand is approximated using a linear relationship [31, 34]. Thus, the real-time price during the i-th time slot, r^i is a linear function of the total load during that interval, l^i and is given by:

$$r^i = r(l^i) = k_0 + k_1\, l^i \quad , \quad \forall i \in \mathbf{I} \tag{5}$$

where k_0 and k_1 are positive real numbers denoting the intercept and slope of the linear relationship, respectively. These coefficients are assigned values that give an average price comparable with other tariffs. Here, $k_0 = 2.3 \times 10^{-3}$ €/kWh and $k_1 = 2.76 \times 10^{-3}$ €/kWh/kW, such that the average price for base load (≈ 0.225 €/kWh) is comparable with that in Spain at present[3].

The total energy cost for the system during the i-th time slot, C_S^i is given by the relation:

$$C_S^i = C_B^i + C_{EV}^i \tag{6}$$

where, C_B^i denotes the energy cost incurred by the base load and C_{EV}^i is the EV charging cost. These costs can be estimated using (7) and (8), in which the price function from (5) is integrated over the corresponding loading limits and multiplied with the interval duration.

$$C_B^i = \left(\int_0^{L_B^i} r(l)\, dl \right) \Delta t \tag{7}$$

[3]Eurostat. Electricity price statistics [online]. Website https://ec.europa.eu/eurostat [accessed 18 July 2021].

$$C_{EV}^{i} = \left(\int_{L_B^i}^{L_{DT}^i} r(l)\, dl \right) \Delta t \tag{8}$$

3. Electric vehicle charging schemes

Two charging schemes are considered in this study: 1) dumb charging, in which EV charging is unaffected by electricity price and 2) smart charging, in which EV charging is regulated to minimize the charging cost. Although, the same EV charging parameters such as energy requirement and plug-in duration are considered in both charging schemes, the charging load applied on the system is considerably different, as explained below.

3.1. Dumb charging scheme

In dumb charging, the vehicles are allowed to charge at the maximum possible rate of P^{max} as soon as they are plugged-in, irrespective of the electricity price. The charging continues until the battery is fully charged or the vehicle departs, whichever occurs first. In this study, the parking time of each EV is greater than the time required for full charge. Thus, the EVs continue to draw energy until they are fully charged.

Under dumb charging, there is no control over the number of plugged-in EVs and the subsequent charging load on the system. The EV charging load at any interval is equal to:

$$L_{EV}^{i} = \sum_{n \in \mathbf{N}} s_n^i \cdot e_n^i \cdot P^{max} \quad , \quad \forall i \in \mathbf{I} \tag{9}$$

where s_n^i and e_n^i are given by (2) and (3) respectively, and $P^{max} = 3$ kW.

3.2. Smart charging scheme

Under SC, the DSO optimizes EV charging with the objective of charging-cost minimization. The optimal charging schedule determines the intervals during which a plugged-in EV is allowed to charge and the power at which it must do so. Therefore, although the number of EVs plugging in remains random, the charging load applied on the network does not; it is maintained at the optimal value that gives the lowest charging cost. The methodology for determining the optimal charging schedule is explained below.

3.2.1. Nomenclature

The following variables are used in the problem formulation of the SC algorithm-

C_{EV}^{day} - total charging cost incurred over the day

C_{EV}^{i} - charging cost incurred during the i-th interval

L_B^i - base load during the i-th interval

L_{DT}^i - distribution transformer loading during the i-th interval

s_n^i - charging status of the n-th EV during the i-th interval

e_n^i - energy requirement status of the n-th EV during the i-th interval

p_n^i - charging power of the n-th EV during the i-th interval

$E_n^{initial}$ - energy available in the battery of the n-th EV at arrival time

E_n^{final} - energy available in the battery of the n-th EV at departure time

$E_n^{desired}$ - energy desired by the n-th EV's user at departure time
$E_n^{capacity}$ - energy storage capacity of the n-th EV's battery
P^{max} - maximum power rating of EV charger
η_n - power conversion efficiency of the n-th EV's charger.

3.2.2. Problem formulation

The total charging cost over a day, C_{EV}^{day} can be obtained by summing the EV charging cost incurred during each time slot over the entire day, i.e.

$$C_{EV}^{day} = \sum_{i \in \mathbf{I}} C_{EV}^{i} \tag{10}$$

where the charging cost per slot, C_{EV}^{i} can be calculated from (8) as:

$$\begin{aligned} C_{EV}^{i} &= \left(\int_{L_B^i}^{L_{DT}^i} r(l)\, dl \right) \Delta t = \left(\int_{L_B^i}^{L_{DT}^i} (k_0 + k_1 l)\, dl \right) \Delta t \\ &= \left[\left(k_0 L_{DT}^i + \frac{k_1}{2} (L_{DT}^i)^2 \right) - \left(k_0 L_B^i + \frac{k_1}{2} (L_B^i)^2 \right) \right] \Delta t \end{aligned} \tag{11}$$

The objective of the smart charging algorithm is to find the optimal charging power p_n^{i*} for each EV $n (\forall n \in \mathbf{N})$ and the resulting optimal charging load L_{EV}^{i*} during each time slot $i\,(\forall i \in \mathbf{I})$ that will minimize the total cost of charging EVs for the day. Mathematically, the charging-cost minimization problem can be formulated as:

$$\min \sum_{i \in \mathbf{I}} \left[\left(k_0 L_{DT}^i + \frac{k_1}{2} (L_{DT}^i)^2 \right) - \left(k_0 L_B^i + \frac{k_1}{2} (L_B^i)^2 \right) \right] \tag{12}$$

subject to the following constraints:

$$L_{DT}^i = L_B^i + \sum_{n \in \mathbf{N}} (s_n^i\, e_n^i\, p_n^i)\ ,\ \forall n \in \mathbf{N}, \forall i \in \mathbf{I} \tag{13}$$

$$E_n^{final} \ \geq \ E_n^{desired}\ ,\ \forall n \in \mathbf{N} \tag{14}$$

$$E_n^{initial} \leq E_n^{final} \leq E_n^{capacity}\ ,\ \forall n \in \mathbf{N} \tag{15}$$

$$0 \leq p_n^i \leq P^{max}\ ,\ \forall n \in \mathbf{N}, \forall i \in \mathbf{I} \tag{16}$$

where

$$E_n^{final} = E_n^{initial} + \sum_{i \in \mathbf{I}} \eta_n (s_n^i\, e_n^i\, p_n^i)\, \Delta t. \tag{17}$$

In the above optimization problem, (12) represents the objective function to be minimized. The objective function is a is a convex function that depends on transformer loading, L_{DT} and the base load, L_B of the system. The Δt term from (11) has been omitted in (12), as it is a constant and cannot affect the minimization process. The relationship between L_{DT}^i, L_B^i and the charging power of individual EVs, p_n^i is given in (13).

Equation (14) represents the final energy constraint which specifies that the final battery energy at departure, E_n^{final} should be equal to or greater than the user-desired level, $E_n^{desired}$. The final energy can be computed by adding the initial energy at plug-in, $E_n^{initial}$ with the total energy transferred subsequently as shown in (17). The final battery energy is constrained by (15) to prevent overcharging beyond rated capacity, $E_n^{capacity}$. Furthermore, as V2G operation is neglected, battery energy can never drop below its initial value. Constraint (16) gives the limits of p_n^i between which it is assumed to be continuously variable. The charging power cannot exceed the maximum rating of the charger. The lower bound is set to zero as negative power flow (V2G) is not considered.

In the problem formulation presented above, the objective function (12) is convex and all the constraints are linear. Therefore, the charging-cost minimization problem is a convex optimization problem, that can be solved efficiently with the interior point method [34]. The solution provides the optimal charging schedule for EVs, from which the optimal EV charging load on the system can be calculated as:

$$L_{EV}^{i*} = \sum_{n \in \mathbf{N}} s_n^i \cdot e_n^i \cdot p_n^{i*} \quad , \quad \forall i \in \mathbf{I} \tag{18}$$

where s_n^i and e_n^i are given by (2) and (3) respectively, and p_n^{i*} is the optimal power at which the n-th EV should charge during the i-th interval, so that the total charging cost will be minimum.

3.3. Comparison of charging schemes

The charging power profile of a single EV (which happens to be of Chevrolet Volt make) under both charging schemes is compared in Figure 1. At the time of plug in (7:00 pm), 6.7 kWh of energy (42% of capacity) is available in the vehicle battery. The vehicle owner expects the vehicle to be charged to its capacity (16 kWh) by the time of departure (8:15 am). Under dumb charging, the EV is allowed to charge at the maximum rating (3 kW) as soon as it is plugged-in, even though the electricity price tends to be higher during this (evening) time of the day. Although the battery requirement is 9.3 kWh, the charger ends up consuming 10.5 kWh owing to power conversion losses (88.5% efficiency). At the rate of 3 kW, the required energy can be delivered in 3.5 hours and the EV is fully charged by 10:30 pm.

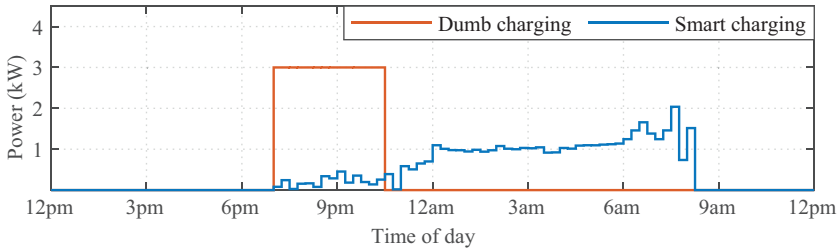

Figure 1. Comparison of charging-power profile of an EV.

However, under SC the same energy is transferred over a much longer duration and the vehicle continues to charge until the time of departure. The charging power is especially small during the initial stages as the prices are higher during this peak-load time. The average charging power has been reduced from 3 kW to 0.82 kW signifying a much smaller impact on transformer loading despite transferring the same amount of energy. An added benefit of SC is the slower degradation of EV battery when compared with dumb charging. The

longer battery life can be attributed to the use of lower charging powers and the lower duration of time spent in fully charged condition [35].

The impact of the two EV charging schemes on DT loading is analyzed next. Dumb charging raises the peak load from 143.08 kVA (under base load) to 255.97 kVA, leaving the 160 kVA rated DT significantly overloaded for an extended duration, as evident from Figure 2. The SC algorithm is able to reduce the peak load to 143.08 kVA, which is within its rated capacity of 160 kVA. The 44% reduction in peak load is more than double of that achieved in [11, 23] and is comparable to that in [6, 10]. Furthermore, as a consequence of shifting EV charging to off-peak hours, the loading profile is much flatter, which implies lower line losses and higher distribution efficiency [36].

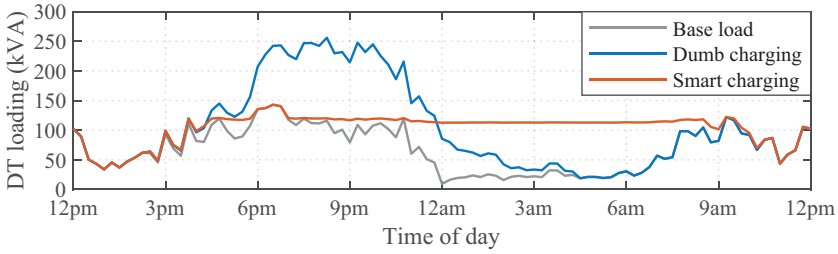

Figure 2. Transformer loading under different scenarios.

4. Analysis of distribution transformer aging

Having analyzed the effect of EVs on DT loading, the next step is to estimate their impact on DT aging. Typically, insulation is the first component to fail within a transformer and the estimated life of a DT is primarily a function of insulation degradation [20]. The state of insulation is governed by the transformer's internal temperature, which has a nonuniform distribution. As a result, the aging effect is evaluated considering the hottest-spot temperature (HST), which corresponds to the point on the winding where the highest temperature and the greatest insulation degradation occurs [5]. The IEEE standard C57.91 [37] has defined the following method for estimating the different temperatures within an oil-immersed transformer such as winding HST and top-oil temperature, which depend on transformer loading and ambient temperature.

The transformer winding's HST at the i-th time slot, Θ^i_{HST} can be determined using:

$$\Theta^i_{HST} = \Theta^i_A + \Delta\Theta^i_{TO} + \Delta\Theta^i_{HST}, \tag{19}$$

where Θ^i_A is the ambient temperature, $\Delta\Theta^i_{TO}$ is the top-oil temperature rise over the ambient temperature, and $\Delta\Theta^i_{HST}$ is the rise in winding HST over the top-oil temperature during the interval. The value of $\Delta\Theta^i_{TO}$ in (19) can be calculated as:

$$\Delta\Theta^i_{TO} = \Delta\Theta^{i-1}_{TO} + (\Delta\Theta_{TO,u} - \Delta\Theta^{i-1}_{TO})(1 - e^{-\Delta t/\tau^{TO}}), \tag{20}$$

where $\Delta\Theta_{TO,u}$ is the ultimate top-oil rise over the ambient temperature and τ^{TO} is the top-oil time constant. The value of $\Delta\Theta^i_{HST}$ in (19) can be calculated as:

$$\Delta\Theta^i_{HST} = \Delta\Theta^{i-1}_{HST} + (\Delta\Theta_{HST,u} - \Delta\Theta^{i-1}_{HST})(1 - e^{-\Delta t/\tau^{W}}), \tag{21}$$

where $\Delta\Theta_{HST,u}$ is the ultimate HST rise over the top-oil temperature and τ^W is the winding time constant.

The ultimate values of top-oil and HST rise can be calculated using (22) and (23), respectively.

$$\Delta\Theta^i_{TO,u} = \Delta\Theta_{TO,r}\left(\frac{k_i^2 R+1}{R+1}\right)^n \tag{22}$$

$$\Delta\Theta_{HST,u} = \Delta\Theta_{HST,r}\left(k_i^{2m}\right), \tag{23}$$

where $\Delta\Theta_{TO,r}$ is the temperature rise of top-oil over ambient at the rated load, $\Delta\Theta_{HST,r}$ is the HST rise over top-oil at the rated load, k_i is the ratio of the transformer load at the i-th interval (L^i_{DT}) to its rated capacity (160 kVA), R is the ratio between the losses at rated load and at no load, and m and n are the cooling parameters of the transformer. The values of these parameters for a typical 160 kVA DT [23] are given in Table 2. By substituting these values in the above equations, the values of HST under different DT loading can be determined.

Table 2. Thermal model parameters of a typical 160 kVA DT [23].

Parameter	τ^{TO}	τ^W	$\Delta\Theta_{TO,r}$	$\Delta\Theta_{HST,r}$	R	m	n
Value	3 h	5 min	55 °C	25 °C	5	0.8	0.8

As the HST rises with transformer loading, the transformer ages at a faster rate. The rate of aging can be quantified using the accelerated aging factor F_{AA}, which is a measure of how quickly the transformer insulation degrades under actual conditions, relative to the degradation at rated HST conditions, which is considered as 110° C. For transformer operation above this reference value, F_{AA} will be greater than one indicating an accelerated aging. F_{AA} can be expressed as an exponential function of Θ_{HST}, as given below [37]:

$$F_{AA} = \exp\left(\frac{15000}{273+110} - \frac{15000}{\Theta_{HST}+273}\right). \tag{24}$$

According to (24), when $\Theta_{HST} = 110°\mathrm{C}$, accelerated aging factor, $F_{AA} = e^0 = 1$, which corresponds to normal aging that occurs at the HST of 110° C. For HST below this value, the transformer ages at a lower than normal rate $(0 < F_{AA} < 1)$. For values above 110° C, the transformer ages at an exponentially higher rate $(F_{AA} \gg 1)$.

The HST of the transformer varies over the day with changes in loading and ambient temperature. The accelerated aging factor, in turn varies as a function of HST throughout the day. Thus, there is a need to express the net amount of aging undergone by the transformer during the entire period under study. The equivalent aging factor was defined for this purpose [37] and its value for the day under study can be calculated as:

$$F_{EQ} = \frac{\sum_{i=1}^{96} F^i_{AA}\Delta t}{\sum_{i=1}^{96}\Delta t}. \tag{25}$$

The value of F_{EQ} represents the transformer's equivalent aging (in days) relative to the normal aging, which is taken as 1 day for a well-dried, oxygen-free unit operating at 110° C.

5. Results and analysis

In this section, the impacts of dumb and smart charging schemes on charging cost and transformer aging are compared. The SC schedule was estimated using the CVX package[4] in MATLAB. The thermal model of the DT was implemented in MATLAB for estimating the HST and aging factor. The test system was simulated in OpenDSS[5], which provides load-flow solution for large-scale distribution networks by solving the system admittance equation using modified augmented nodal analysis. The nodal analysis technique, which has good convergence characteristics and high computational performance, is capable of handling arbitrary network topologies in the multiphase and unbalanced context [38].

The real-time price of electricity under the three loading scenarios is compared in Figure 3. It is clear that dumb charging is subjected to much higher prices when compared with the other two scenarios. The prices are the highest during the evening hours, when majority of the EV users return home from work and plug-in their vehicles for charging. In contrast, SC delays EV charging from the evening hours to the off-peak hours around the dawn of the following day.

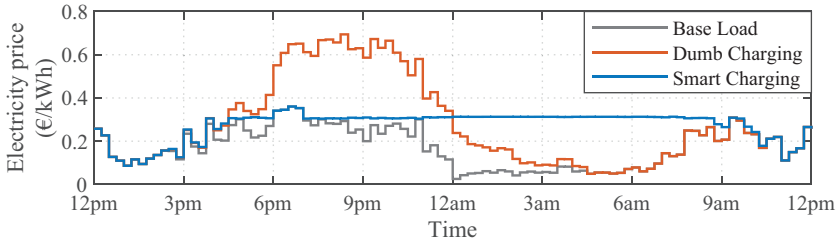

Figure 3. Electricity price under different scenarios.

The combined action of peak-shaving and valley-filling leads to a flatter load profile (as evident in Figure 2) and steady prices. SC is able to reduce the EV charging cost from 421.39 € to 266.61 €. Having thus realized the primary objective of charging-cost minimization, the impact on DT aging is addressed next. The ambient temperature of Madrid, the capital city of Spain is considered in this study. The temperature profile, $\Theta_A^i (\forall i \in \mathbf{I})$ in Madrid during two days: one in July, representing summer and the other in December, corresponding to winter were utilized in this study. The temperature profiles[6] are illustrated in Figure 4.

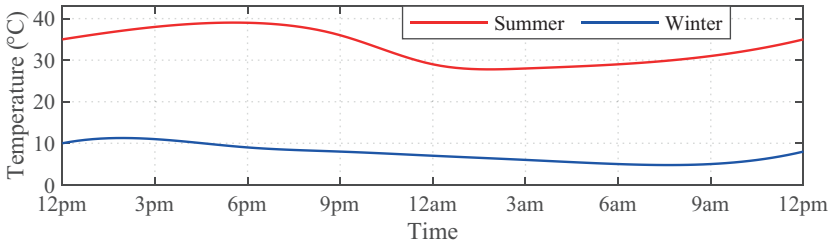

Figure 4. Ambient temperature profile.

The HST and aging factor of the DT under dumb charging during the two seasons are compared in Figure

[4]CVX: Matlab software for disciplined convex programming [online]. Website http://cvxr.com/cvx [accessed 11 June 2021].
[5]EPRI. OpenDSS Program [online]. Website http://sourceforge.net/projects/electricdss [accessed 11 June 2021].
[6]World Weather Online. Madrid Historical Weather [online]. Website https://www.worldweatheronline.com/madrid-weather-history/madrid/es.aspx [accessed 11 June 2021].

5. During summer, the winding HST and aging factor are significantly higher with peak values of 167.26 °C and 162.99, respectively. Due to the lower ambient temperature during winter, the peak values of HST and aging factor drop to 141.34 °C and 19.35 respectively. The equivalent aging factor under summer is found to be 12.48 which implies that the DT ages nearly twelve and a half times as fast as it would normally have. During winter, although the aging is faster than normal, the rate of acceleration is much smaller at 1.22.

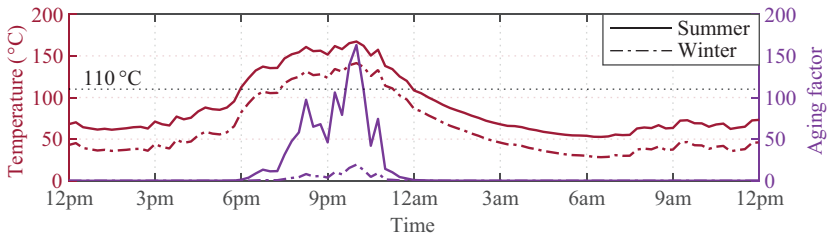

Figure 5. Variation in HST and aging factor of transformer under dumb charging.

The impact of SC on the HST and aging factor of the DT during the two seasons are compared in Figure 6. Due to regulated EV charging that eliminates DT overloads, the HST never exceeds 110° C resulting in a slower-than-normal aging. This is also reflected in the accelerated aging factor which never exceeds 1 (the value corresponding to normal aging) with peak values of 0.19 and 0.01 during summer and winter, respectively. The equivalent aging factors of 0.046 (summer) and 0.004 (winter) imply a much longer service life under SC. The longer life of the DT can be attributed to its cooler operation on account of controlled EV charging by the SC algorithm.

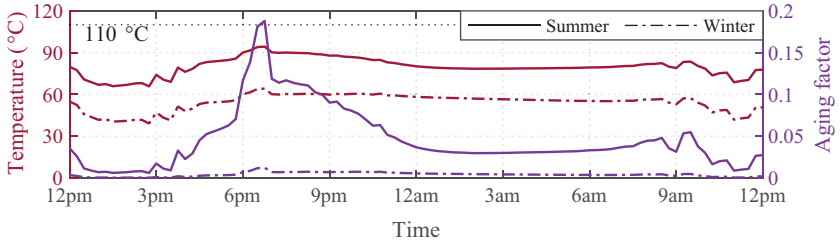

Figure 6. Variation in HST and aging factor of transformer under smart charging.

5.1. Summary

The benefits of the SC method presented in this paper can be appreciated from Table 3. The charging cost was reduced by 36.73% from what it would have been under dumb charging. The cost saving will act as an incentive for EV owners to relinquish the charging control of their vehicles and participate in centralized charging schemes. From the DSO's perspective, SC is able to prevent DT overload by reducing the peak load by 44%. It can be observed from the mean HST values that EV charging in general raises the operating temperature within the DT. Due to the absence of overloads, SC leads to a cooler operation by 9.7% and 13.6% during summer and winter, respectively. By reducing the peak HST by 43.6% (summer) and 54.6% (winter), SC is able to restrict HST below 110 °C and achieve aging-factor reduction in excess of 99% under both seasons.

Table 3. Summary of simulation results.

Parameter	No EV charging	Dumb EV charging	Smart EV charging
EV charging cost (€)	0	421.39	266.61
Peak transformer load (kVA)	143.08	255.97	143.08
Summer season			
Peak HST (°C)	91.06	167.26	94.32
Mean HST (°C)	64.52	88.39	79.82
Peak aging factor	0.13	162.99	0.19
Equivalent aging factor	0.02	12.48	0.05
Winter season			
Peak HST (°C)	60.95	141.34	64.22
Mean HST (°C)	38.89	62.77	54.20
Peak aging factor	0.003	19.35	0.01
Equivalent aging factor	0.0004	1.22	0.004

6. Conclusion

Uncontrolled or dumb EV charging can negatively affect the peak load, network utilization and transformer aging. In this scenario, having identified the need for regulated EV charging, a smart charging scheme was developed. With smart charging, the DSO seeks to accommodate the EV charging loads by optimally scheduling them to achieve a certain objective. The target of the charge scheduling scheme in this study was to minimize the charging cost incurred by EV owners, which makes it worthwhile for them to participate in such charge management schemes. The cost minimization was performed with respect to a real-time pricing tariff in which the electricity price is modeled as a linear function of the system demand. The linear dependence ensures that charging-cost minimization leads the way for network decongestion. In the optimal charging schedule, EV charging is shifted from peak load hours (peak shaving) to the off-peak hours (valley filling). Peak shaving prevents transformer overloads and its accelerated aging, while valley filling ensures better utilization of the network infrastructure. Thus, with smart charging the primary concerns of both the EV owners and the DSO, with regard to energy costs and transformer life have been addressed. Future research could seek to incorporate bidirectional smart charging based on vehicle-to-grid or vehicle-to-home technology into the aging study.

References

[1] García-Villalobos J, Zamora I, San Martín JI, Asensio FJ, Aperribay V. Plug-in electric vehicles in electric distribution networks: A review of smart charging approaches. Renewable and Sustainable Energy Reviews. 2014; 38: 717-731. doi: 10.1016/j.rser.2014.07.040

[2] Fischer D, Harbrecht A, Surmann A, McKenna R. Electric vehicles' impacts on residential electric local profiles – A stochastic modelling approach considering socio-economic, behavioural and spatial factors. Applied Energy. 2019; 233: 644-658. doi: 10.1016/j.apenergy.2018.10.010

[3] Deilami S, Masoum AS, Moses PS, Masoum MAS. Real-Time Coordination of Plug-In Electric Vehicle Charging in Smart Grids to Minimize Power Losses and Improve Voltage Profile. IEEE Transactions on Smart Grid. 2011; 2 (3): 456-467. doi: 10.1109/TSG.2011.2159816

[4] Kasturi K, Nayak MR. Assessment of techno-economic benefits for smart charging scheme of electric vehicles in residential distribution system. Turkish Journal of Electrical Engineering & Computer Sciences 2019; 27 (2): 685-696. doi: 10.3906/elk-1801-34

[5] Affonso CM, Kezunovic M. Probabilistic Assessment of Electric Vehicle Charging Demand Impact on Residential Distribution Transformer Aging. In: 2018 IEEE International Conference on Probabilistic Methods Applied to Power Systems; Edmonton, AB, Canada; 2018. pp. 1-6.

[6] Erdogan N, Erden F, Kisacikoglu M. A fast and efficient coordinated vehicle-to-grid discharging control scheme for peak shaving in power distribution system. Journal of Modern Power Systems and Clean Energy. 2018; 6 (3): 555-566. doi: 10.1007/s40565-017-0375-z

[7] Arnaudo M, Topel M, Laumert B. Vehicle-to-grid for peak shaving to unlock the integration of distributed heat pumps in a Swedish neighborhood. Energies. 2020; 13 (7): 1705. doi: 10.3390/en13071705

[8] Xu H, Xia X, Liang W, Zhang L, Dong G, Yan Y, Yu B, Ouyang F, Zhu W, Liu H. Optimal charging of large-scale electric vehicles over extended time scales. Electrical Engineering. 2020; 102 (1): 461-9. doi: 10.1007/s00202-019-00887-6

[9] Mehta R, Srinivasan D, Khambadkone AM, Yang J, Trivedi A. Smart charging strategies for optimal integration of plug-in electric vehicles within existing distribution system infrastructure. IEEE Transactions on Smart Grid. 2018; 9 (1): 299-312. doi: 10.1109/TSG.2016.2550559

[10] Kisacikoglu MC, Erden F, Erdogan N. Distributed Control of PEV Charging Based on Energy Demand Forecast. IEEE Transactions on Industrial Informatics. 2018; 14 (1): 332-341. doi: 10.1109/TII.2017.2705075

[11] Hashim MS, Yong JY, Ramachandaramurthy VK, Tan KM, Mansor M, Tariq M. Priority-based vehicle-to-grid scheduling for minimization of power grid load variance. Journal of Energy Storage. 2021; 39:102607. doi: 10.1016/j.est.2021.102607

[12] Suyono H, Rahman MT, Mokhlis H, Othman M, Illias HA, Mohamad H. Optimal scheduling of plug-in electric vehicle charging including time-of-use tariff to minimize cost and system stress. Energies. 2019; 12 (8): 1500. doi: 10.3390/en12081500

[13] Crozier C, Deakin M, Morstyn T, McCulloch M. Coordinated electric vehicle charging to reduce losses without network impedances. IET Smart Grid. 2020; 3 (5): 677-85. doi: 10.1049/iet-stg.2019.0216

[14] Islam MR, Lu H, Hossain J, Li L. Multiobjective optimization technique for mitigating unbalance and improving voltage considering higher penetration of electric vehicles and distributed generation. IEEE Systems Journal. 2020; 14 (3): 3676-86. doi: 10.1109/JSYST.2020.2967752

[15] Boonseng T, Sangswang A, Naetiladdanon S, Gurung S. A New Two-Stage Approach to Coordinate Electrical Vehicles for Satisfaction of Grid and Customer Requirements. Applied Sciences. 2021; 11 (9): 3904. doi: 10.3390/app11093904

[16] Shi Y, Tuan HD, Savkin AV, Duong TQ, Poor HV. Model predictive control for smart grids with multiple electric-vehicle charging stations. IEEE Transactions on Smart Grid. 2018; 10 (2): 2127-36. doi: 10.1109/TSG.2017.2789333

[17] Bakhshinejad A, Tavakoli A, Moghaddam MM. Modeling and simultaneous management of electric vehicle penetration and demand response to improve distribution network performance. Electrical Engineering. 2021; 103 (1): 325-40. doi: 10.1007/s00202-020-01083-7

[18] Patil H, Kalkhambkar VN. Charging cost minimisation by centralised controlled charging of electric vehicles. International Transactions on electrical Energy Systems. 2020; 30 (2): e12226. doi: 10.1002/2050-7038.12226

[19] Islam JB, Rahman MT, Mokhlis H, Othman M, IZAM TF et al. Combined analytic hierarchy process and binary particle swarm optimization for multiobjective plug-in electric vehicles charging coordination with time-of-use tariff. Turkish Journal of Electrical Engineering & Computer Sciences. 2020; 28 (3): 1314-1330. doi: 10.3906/elk-1907-189

[20] Hilshey AD, Hines PDH, Rezaei P, Dowds JR. Estimating the Impact of Electric Vehicle Smart Charging on Distribution Transformer Aging. IEEE Transactions on Smart Grid. 2013; 4 (2): 905-913. doi: 10.1109/TSG.2012.2217385

[21] Gong Q, Midlam-Mohler S, Marano V, Rizzoni G. Study of PEV Charging on Residential Distribution Transformer Life. IEEE Transactions on Smart Grid. 2012; 3 (1): 404-412. doi: 10.1109/TSG.2011.2163650

[22] Turker H, Bacha S, Hably A. Rule-Based Charging of Plug-in Electric Vehicles (PEVs): Impacts on the Aging Rate of Low-Voltage Transformers. IEEE Transactions on Power Delivery. 2014; 29 (3): 1012-1019. doi: 10.1109/TPWRD.2013.2292066

[23] Razeghi G, Zhang L, Brown T, Samuelsen S. Impacts of plug-in hybrid electric vehicles on a residential transformer using stochastic and empirical analysis. Journal of Power Sources. 2014; 252: 277-285. doi: 10.1016/j.jpowsour.2013.11.089

[24] Shrestha GB, Ang SG. A study of electric vehicle battery charging demand in the context of Singapore. In: 2007 International Power Engineering Conference; Singapore; 2007. pp. 64-69.

[25] Qian K, Zhou C, Yuan Y. Impacts of high penetration level of fully electric vehicles charging loads on the thermal ageing of power transformers. International Journal of Electrical Power & Energy Systems. 2015; 65: 102-112. doi: 10.1016/j.ijepes.2014.09.040

[26] Sarker MR, Olsen DJ, Ortega-Vazquez MA. Co-Optimization of Distribution Transformer Aging and Energy Arbitrage Using Electric Vehicles. IEEE Transactions on Smart Grid. 2017; 8 (6): 2712-2722. doi:10.1109/TSG.2016.2535354

[27] Affonso C de M, Kezunovic M. Technical and Economic Impact of PV-BESS Charging Station on Transformer Life: A Case Study. IEEE Transactions on Smart Grid. 2019 ; 10 (4): 4683-4692. doi: 10.1109/TSG.2018.2866938

[28] Godina R, Rodrigues EMG, Matias JCO, Catalão JPS. Smart electric vehicle charging scheduler for overloading prevention of an industry client power distribution transformer. Applied Energy. 2016; 178: 29-42. doi: 10.1016/j.apenergy.2016.06.019

[29] Chen N. Electric Vehicle Charging in Smart Grid: Optimality and Valley-Filling Algorithms. IEEE Journal of Selected Topics in Signal Processing. 2014; 8 (6): 1073-1083. doi: 10.1109/JSTSP.2014.2334275

[30] O'Connell A, Flynn D, Keane A. Rolling Multi-Period Optimization to Control Electric Vehicle Charging in Distribution Networks. IEEE Transactions on Power Systems. 2014; 29 (1): 340–348. doi: 10.1109/TPWRS.2013.2279276

[31] Veldman E, Verzijlbergh RA. Distribution Grid Impacts of Smart Electric Vehicle Charging From Different Perspectives. IEEE Transactions on Smart Grid. 2015; 6 (1): 333-42. doi: 10.1109/TSG.2014.2355494

[32] Cao Y, Tang S, Li C, Zhang P, Tan Y et al. An Optimized EV Charging Model Considering TOU Price and SOC Curve. IEEE Transactions on Smart Grid. 2012; 3 (1): 388-93. doi: 10.1109/TSG.2011.2159630

[33] Jin C, Tang J, Ghosh P. Optimizing Electric Vehicle Charging: A Customer's Perspective. IEEE Transactions on Vehicular Technology. 2013; 62 (7): 2919–2927. doi: 10.1109/TVT.2013.2251023

[34] He Y, Venkatesh B, Guan L. Optimal Scheduling for Charging and Discharging of Electric Vehicles. IEEE Transactions on Smart Grid. 2012 ; 3 (3): 1095-1105. doi: 10.1109/TSG.2011.2173507

[35] Ahmadian A, Sedghi M, Mohammadi-ivatloo B, Elkamel A, Golkar MA et al. Cost-benefit analysis of V2G implementation in distribution networks considering PEVs battery degradation. IEEE Transactions on Sustainable Energy. 2018; 9 (2): 961-70. doi: 10.1109/TSTE.2017.2768437

[36] Sortomme E, Hindi MM, MacPherson SDJ, Venkata SS. Coordinated Charging of Plug-In Hybrid Electric Vehicles to Minimize Distribution System Losses. IEEE Transactions on Smart Grid. 2011; 2 (1): 198-205. doi: 10.1109/TSG.2010.2090913

[37] IEEE Standard C57.91-2011. IEEE Guide for Loading Mineral-Oil-Immersed Transformers and Step Voltage Regulators. 2012.

[38] Kocar I, Mahseredjian J, Karaagac U, Soykan G, Saad O. Multiphase load-flow solution for large-scale distribution systems using MANA. IEEE Transactions on Power Delivery. 2013; 29 (2): 908-15. doi:10.1109/TPWRD.2013.2279218